International Journal of Environmental Sciences
ISSN: 2229-7359
Vol. 11 No. 5, 2025
https://theaspd.com/index.php

Dual Solutions of Nanofluid Boundary Layer Flow Over an Inclined Stretching Sheet with Mixed Convection Slip Boundary Condition

Shefali Jauhri[1], Prof Upendra Mishra[2]
[1]Department of Mathematics, Invertis University, Rajau Paraspur, National Highway NH 30, Bareilly, Lucknow, Uttar Pradesh 243123, Shefali.jauhri3@gmail.com
[2]Department of Mathematics, Amity University Rajasthan, NH-11 C, Kant Kalwar, Delhi-Jaipur Highway, Near Achrol Village, Jaipur, India, umishra@jpr.amity.edu

Abstract
This study explores heat transfer in nanofluid boundary layers over a stretching sheet, incorporating the effects of a magnetic field. The analysis considers thermal slip and second-order velocity slip boundary conditions. Using a similarity transformation, the governing partial differential equations are converted into ordinary differential equations, which are then numerically solved using the fourth-order Runge-Kutta (RK4) method. The impact of key governing parameters on temperature, nanoparticle concentration, dimensionless velocity, and the skin friction coefficient is examined. A dual solution is identified for velocity profiles, skin friction, and local skin friction coefficients, revealing a significant dependence on the second-order velocity slip parameter. The effects of other parameters are also illustrated graphically for comprehensive understanding.
Keywords: *Second-order velocity slip, EMHD, Nanofluid, Similarity transformation, Dual solution.*

INTRODUCTION

The study of incompressible viscous fluid flow over a stretching sheet with slip boundary conditions has profound relevance in numerous industrial and engineering processes. These processes include the cooling of nuclear reactors, metallic plates, and polymers, wire drawing, paper production, glass fibre manufacturing, and heat transfer mechanisms. Compared to molecular-based methods, continuum descriptions with second-order slip boundary conditions provide significant advantages in solving flow and heat transfer problems effectively.

With advancements in modern technology, researchers have increasingly focused on heat transfer phenomena, given their critical role in power generation, nuclear reactor cooling, polymer production, and other industrial operations. Ahmed's study [1] addressed heat flow and suction effects in incompressible viscous fluids over stretched sheets, emphasizing variable thermal conductivity. Aman [2] analyzed the influence of second-order slip in magnetohydrodynamic (MHD) flow on fractional Maxwell fluids, contrasting semi-analytical solutions derived using Laplace transformations.

Bhargava et al. [3] investigated micropolar fluid flow over nonlinearly extending sheets, while Cao [4] modeled colloidal solutions containing nanoparticles such as carbon nanotubes, graphene, and alumina. This study examined forced, free, and mixed convection phenomena under partial slip conditions. Choi [5] pioneered nanofluid research, employing nanoparticles to enhance thermal conductivity. Cortell [6] extended this approach by investigating viscous flows over nonlinearly extending sheets.

Magnetohydrodynamic (MHD) effects were further explored by Fang [7], who analyzed slip flow on porous, linearly stretching sheets, while Ganesh [8] incorporated entropy generation in buoyancy-driven flows under non-linear thermal radiation. Gangadhar et al. [9–10] utilized computational and spectral relaxation methods to study nanofluid boundary layer properties.

Hayat et al. [12–13] explored Jeffrey fluid dynamics in radially stretched nonlinear sheets and exponentially stretched sheets under slip conditions, highlighting the dual significance of Newtonian and Joule heating mechanisms. Subsequent research by Kalidas [17] quantified boundary layer flow of nanofluids over nonlinear permeable sheets, incorporating partial slip conditions.

Khan and Pop [19] introduced boundary layer flow models for nanofluids on stretching sheets, while Song et al. [26] studied the thermal behavior of water and ethylene glycol mixtures containing alumina

and copper nanoparticles. Other researchers, including Sakthivel [24] and Sharma et al. [25], examined the influence of thermal conductivity, porosity, and magnetic parameters on nanofluid flow.
Zeng [29] highlighted the interplay between Darcy and Forchheimer regimes in laminar and nonlinear flows, emphasizing inertial effects. Building on these foundational studies, this research investigates the influence of second-order slip boundary conditions on nanofluid flow and heat transfer over inclined stretching sheets in the presence of a magnetic field.
Research Objectives: This study addresses the following questions to deepen the understanding of nanofluid dynamics under second-order slip conditions:

1. **Significance of Second-Order Velocity Slip Parameter**
   How does increasing the second-order velocity slip parameter influence velocity and temperature profiles in the nanofluid boundary layer?
2. **Impact of Governing Parameters on Heat and Mass Transfer**
   How do key parameters, such as Brownian motion, thermophoresis, and magnetic fields, affect nanofluid flow and heat transfer?
3. **Effect of Inclination Angle on Flow Dynamics**
   What is the impact of increasing the angle of inclination, in conjunction with first- and second-order slip parameters, on velocity and temperature distributions?

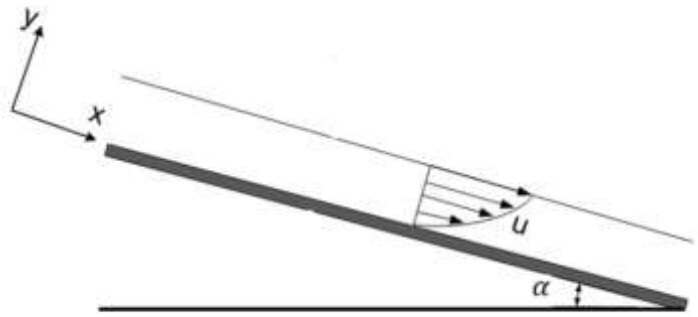

Fig.1. Physical Configuration of Boundary Layer Flow over an Inclined Sheet

1. Mathematical Formulation: In this investigation, we examine an incompressible nanofluid streaming over a sheet that expands with the slip boundary. With the use of Maxwell's equation and the study of EMHD, the extended equation of continuity, equation of momentum, equation of fluid energy, and equation of fluid concentration produced. An inclined sheet is subjected to the electrically conducting viscous incompressible nanofluid flow of mixed convection. The thin plate forms the path of the tangential flow in the X- direction, and the Y- axis is perpendicular to it.

$$\frac{\partial u}{\partial x}+\frac{\partial v}{\partial y}=0 \quad (1)$$

$$u\frac{\partial u}{\partial x}+v\frac{\partial u}{\partial y}=u_\infty\frac{\partial u_\infty}{\partial x}+v_f\frac{\partial^2 u}{\partial y^2}+\frac{\sigma {B_o}^2}{\rho_f}(U-u)+g_x\beta_t(T-T_\infty)sin\alpha+g_x\beta_c(C-C_\infty)sin\alpha+\frac{\sigma B_o E_o}{\rho_f} \quad (2)$$

$$u\frac{\partial T}{\partial x}+v\frac{\partial T}{\partial y}=\frac{k_f}{\rho c_p}\frac{\partial^2 T}{\partial y^2}+\frac{Q_0}{(\rho c_p)_f}(T-T_\infty)+\frac{(\rho c_p)_p}{(\rho c_p)_f}\left[D_B\frac{\partial C}{\partial y}\frac{\partial T}{\partial y}+\frac{D_T}{T_\infty}\left(\frac{\partial T}{\partial y}\right)^2\right]. \quad (3)$$

$$u\frac{\partial C}{\partial x}+v\frac{\partial C}{\partial y}=D_B\frac{\partial^2 C}{\partial y^2}+\frac{D_T}{T_\infty}\left(\frac{\partial^2 T}{\partial y^2}\right) \quad (4)$$

boundary conditions are,

$$\left.\begin{aligned} \mathrm{u} = C_1\mathrm{x} + L_1\frac{\partial u}{\partial y} + L_2\frac{\partial^2 u}{\partial y^2}, v = 0 \\ \mathrm{T} = T_{\dot{w}} + q_1\frac{\partial T}{\partial y} \\ C = C_{\dot{w}} + q_2\frac{\partial C}{\partial y} \end{aligned}\right\} \text{at} \quad y = 0 \tag{5}$$

$$\left.\begin{aligned} u \to 0 \\ T \to T_\infty \\ C \to C_\infty \end{aligned}\right\} \text{as} \;\; y \to \infty \tag{6}$$

In reference of velocity, L_1 and L_2 are slip parameter and kinematic-viscosity is 'ν' and 'C_1' is the constant of proportionality. Here q_1 and q_2 are slip parameters in reference of temperature and concentration. Similarity variables are

$$\xi = y\sqrt{\frac{a}{\nu_f}} \tag{7}$$

$u = axh'(\xi)$ and $v = -\sqrt{a\nu_f}h(\xi)$

The dimensionless temperature and concentration variables are

$t(\xi) = \frac{T-T_\infty}{T_W-T_\infty}, \quad \varphi(\xi) = \frac{c-c_\infty}{c_W-c_\infty}$

T=$T_\infty + Ax\, t(\xi)$ and

c=$c_\infty + Bx\varphi\,(\xi)$ (8)

Using equation (7) and (8) in equations (2), (3) & (4). We get,

$$h''' + hh'' - h'^2 + m(1-h') + G_t t sin\alpha + G_c\varphi sin\alpha - me = 0 \tag{9}$$

$$t'' + Pr[ht' + \lambda t + N_b t'\varphi' + N_t t'^2] + \varepsilon(tt'' + t'^2) = 0 \tag{10}$$

$$\varphi'' + Scf\varphi' + \frac{N_t}{N_b}t'' = 0 \tag{11}$$

The boundary conditions are

$$\left.\begin{aligned} h = S, h' = 1 + \beta_1 h'' + \beta_2 h''' \\ t(\xi) = 1 + \delta_1 t'(\xi) \\ \varphi(\xi) = 1 + \delta_2\varphi'(\xi) \end{aligned}\right\} at\ \xi = 0 \tag{12}$$

$$\left.\begin{aligned} h' \to 0 \\ t \to 0 \\ \varphi \to 0 \end{aligned}\right\} as \;\; \xi \to \infty \tag{13}$$

Where $\beta_1 = L_1\sqrt{a/\nu}$ and $\beta_2 = \frac{a}{\nu}L_2$, are referred to as the 2nd and 3rd order coefficients of slip parameters.$\delta_1 = K_1\sqrt{\frac{a}{\nu}}$ and $\delta_2 = K_2\sqrt{\frac{a}{\nu}}$ are referred to as the slip coefficient of heat transfer and slip coefficient of mass diffusion.

The transfer of heat, in accordance with Ahmed [1], occurs in two components, one of which is caused by a difference in temperature and the other by a variation in thermal conductivity. In equation (10), the term independent of ε, i.e. $t'' + Pr[ht' + \lambda t + N_b t'\varphi' + N_t t'^2]$ is caused by difference in temperature, while the 2nd component, i.e., $\varepsilon(tt'' + t'^2)$, is caused by variable thermal conductivity.

2.1 SKIN FRICTION: The Skin friction coefficient C_f at the surface is defined as,

$$C_f = \frac{\tau}{\frac{1}{2}\rho u^2}\bigg|_{y=0}$$

Where, stress $\tau = \mu\frac{\partial u}{\partial y}$

Hence

$$C_f = \frac{\mu\frac{\partial u}{\partial y}}{\frac{1}{2}\rho u^2}\bigg|_{y=0} = \frac{2f''(0)}{\sqrt{Re}}$$

Therefore,

$$f''(0) = \frac{1}{2}\sqrt{Re}\, C_f$$

2.2 Nusselt Number and Sherwood Number: - The Nusselt number is defined as follows,

$$Nu = \frac{xQ_w}{k_f(T_w - T_\infty)}$$

Similarly, the Sherwood's number is defined as,

$$Sh = \frac{xQ_m}{D_B(C_w - C_\infty)}$$

Here,
$Q_w\ is$ heat flux.
$Q_m is$ mass flux.
Thermal conductivity coefficient is represented by k.
characteristic length is represented by x
By using equation (9) we get,
$\frac{Nu}{Re_x^{1/2}} = -\left[1 + \frac{\varepsilon\theta(0)}{1+\varepsilon\theta(0)}\right]\theta'(0),\ \frac{Sh}{Re_x^{1/2}} = -\phi'(0)$. Where, local Reynolds number $Re_x = \frac{u_w x}{\upsilon}$.

Numerical Solution: -

This study examines the heat conduction-convection system, characterized by a highly non-linear system of partial differential equations (PDEs), making the discovery of an exact solution particularly challenging. To address this, a similarity variable is utilized to transform the non-linear partial differential equation (PDE) into a non-linear ordinary differential equation (ODE). The model has been analyzed using the 4th-order method and the shooting technique. Equations (9–11) encompass the effects of the 2nd-order slip parameter, considering various parameters such as S_c N_b, m, e and P_r. Additionally, the following new variables were introduced: $f_1 = h,\ f_2 = h',\ f_3 = h'',\quad f_4 = t, f_5 = t', f_6 = \varphi, f_7 = \varphi'$
Subsequently, the equations (9-11) become:

$$f_1' = f_2, f_2' = f_3 \quad (14)$$

$$f_3' = -f_1 * f_3 + f_2^2 - M(1 - f_2) - G_t f_4 sin\alpha - G_c f_6 sin\alpha + \text{ME} \quad (15)$$

$$f_4' = f_5 \quad (16)$$

$$f_5' = -\varepsilon\left(f_4 * f_5' + {f_5}^2\right) - Pr * [f_1 * f_5 + \lambda * f_4 + N_b f_5 * f_7 + N_t * f_5^2] \quad (17)$$

$$f_6' = f_7 \quad (18)$$

$$f_7' = -Sc f_1 f_7 + \frac{N_t}{N_b} f_5' \quad (19)$$

With boundary conditions,

$$f = 0, f_2 = 1 + \beta_1 f_3 + \beta_2 f_3' \quad at\ \xi = 0 \quad (20)$$

$$f_2 \to 0\ as\ \ \xi \to \infty$$

$$f_4(0) = 1 + \delta_1 f_5(0), f_6(0) = 1 + \delta_2 f_7(0) \quad (21)$$

$$f_4 \to 0\ as\ \ \xi \to \infty,\ f_6 \to 0\ as\ \ \xi \to \infty$$

Table-1: Comparison of the values of $-$t′ (0) and $-\varphi'$ (0) for different values of N_t and N_b and Gt = Gc = λ =m= e = δ_1 = δ_2 = S = 0 and S_c = P_r = 10 with Khan and Pop [85]

N_t	N_b	$-t'(0)$ Khan & Pop	$-\varphi'(0)$ Khan & Pop	$-t'(0)$ K.L.Hsiao	$-\varphi'(0)$ K.L.Hsiao	$-t'(0)$ Present Result	$-\varphi'(0)$ Present Result
0.1	0.1	0.9524	2.1294	0.9524	2.1294	0.952402	2.129421
0.2	0.1	0.6932	2.2740	0.6932	2.2740	0.693211	2.274012
0.3	0.1	0.5201	2.5286	0.5201	2.5286	0.520113	2.528641
0.4	0.1	0.4026	2.7952	0.4026	2.7952	0.402621	2.795201
0.5	0.1	0.3211	3.0351	0.3211	3.0351	0.321101	3.035103
0.1	0.2	0.5056	2.3819	0.5056	2.3819	0.505612	2.381902
0.1	0.3	0.2522	2.4100	0.2522	2.4100	0.252223	2.410010
0.1	0.4	0.1194	2.3997	0.1194	2.3997	0.119412	2.399652
0.1	0.5	0.0543	2.3836	0.0543	2.3836	0.054301	2.383567

International Journal of Environmental Sciences
ISSN: 2229-7359
Vol. 11 No. 5, 2025
https://theaspd.com/index.php

RESULT AND DISCUSSION:

With a 2nd-order velocity slip parameter, Maxwell fluid flow has been studied across an inclined stretched sheet. To solve the system of nonlinear differential equations (9)-(11) with boundary conditions (12-13), we employed the Runge Kutta fourth-order approach. Physical parameters (e.g., magnetic parameters, 1st and 2nd order velocity slip parameters, heat transfer slip parameter) have been widely investigated to fully understand their influence. Temperature, velocity, concentration profile graphs, and local Nusselt and Sherwood numbers are used to depict the results of this study. Analysis of data in relation to numerous boundaries was carried out using the method described earlier.

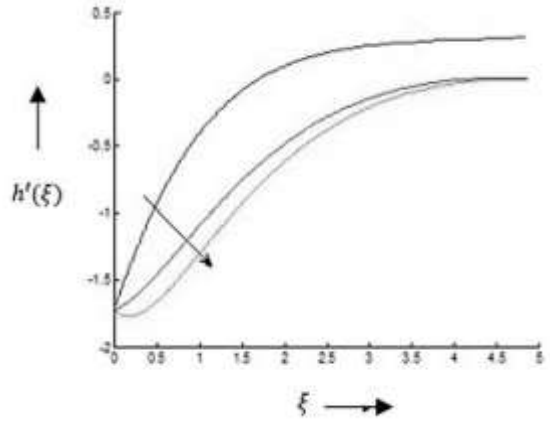

Fig.2(a)

I^{s}t solution of variation of $h'(\xi)$ vs ξ on different values of $\beta_2 = 0.1,0.3,0.5$ with m=e= $N_t = N_b = 0.1$,Pr=1, $G_t = 1, G_c = 0.1$.

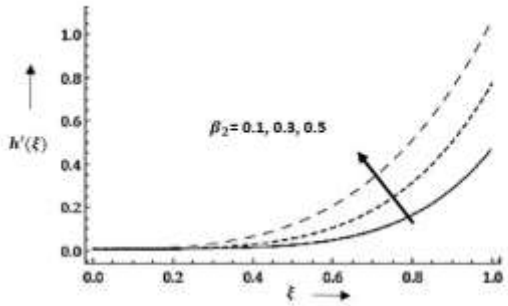

Fig.2(b)

Dual solution of variation of $h'(\xi)$ vs ξ on different values of $\beta_2 = 0.1,0.3,0.5$ with m=e= $N_t = N_b = 0.1$,Pr=1, $G_t = 1, G_c = 0.1$.

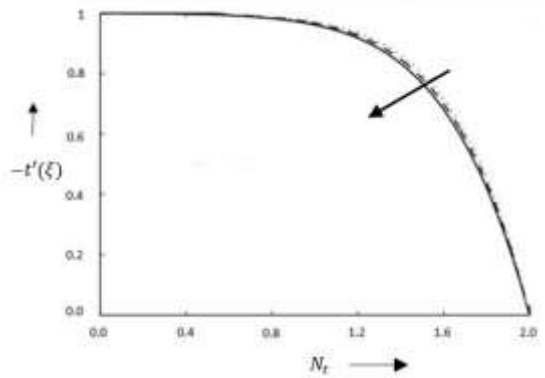

Fig.3(a)

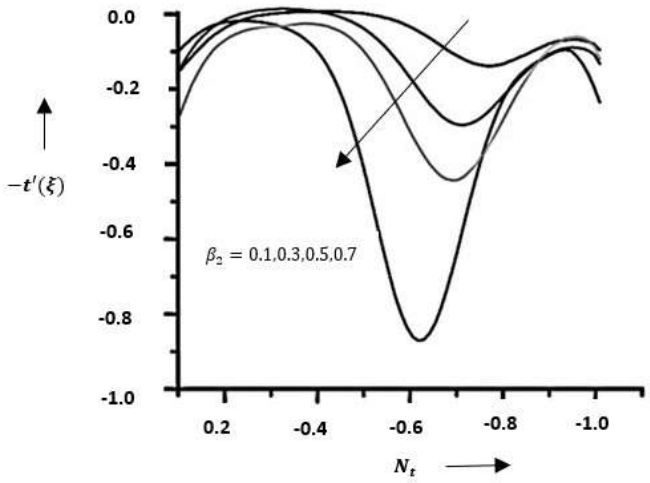

Fig.3(b)
Dual solution of variation of $-t'(\xi)$ vs ξ on different values of $\beta_2 = 0.1,0.3,0.5,0.7$ with m=e= $N_t = N_b = 0.1$,Pr=1, $G_t = 1, G_c = 0.1$.

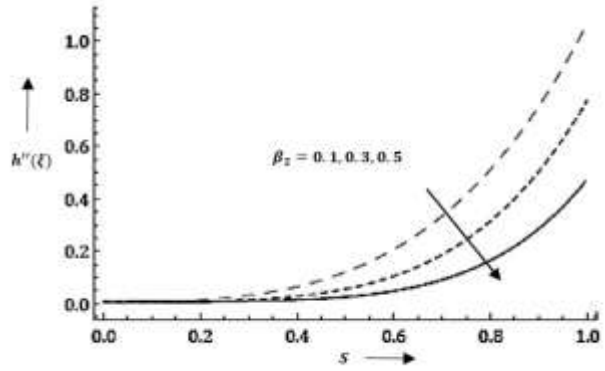

Fig.4(a)

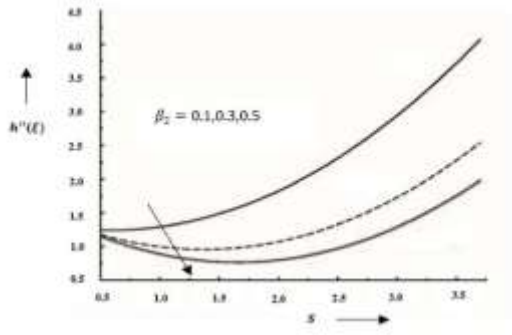

Fig.4(b)
Dual solution of variation of $h''(\xi)$ vs ξ on different values of $\beta_2 = 0.1,0.3,0.5$ with m=e= $N_t = N_b = 0.1$,Pr=1, $G_t = 1, G_c = 0.1$.

Figure 2a and 2b shows the effect of the 2nd-order slip parameter β_2 on the dimensionless velocity. It is observed that the dimensionless velocity decreases in the first solution and increases in second with increasing the values of the 2nd order slip parameter. Similarly, figures 3a,3b & 4a,4b shows the effect of the 2nd order slip parameter β_2 on the dimensionless reduced Nusselt number $-t'(0)$. and skin friction $-h''(0)$. It is observed that the dimensionless reduced Nusselt number

increasing in both solutions while dimensionless skin friction in decreasing in both solutions.

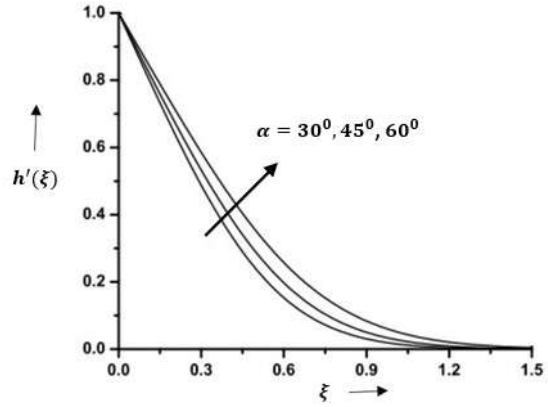

Fig.5
Variation of $h'(\xi)$ vs ξ on different values of $\alpha = 30^0, 45^0, 60^0$ with m=e= $N_t = N_b = 0.1$, Pr=1, $G_t = 1, G_c = 0.1$.

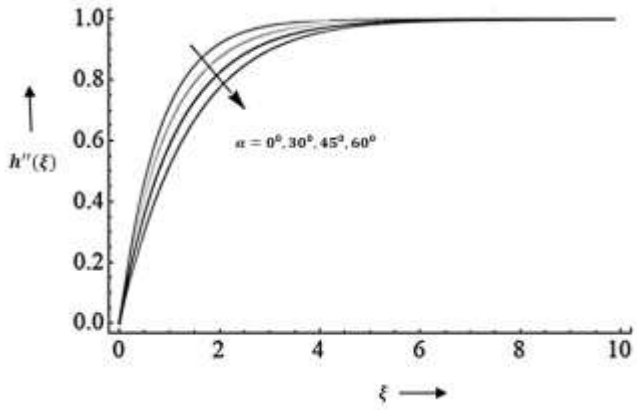

Fig.6
Variation of $h''(\xi)$ vs ξ on different values of $\alpha = 30^0, 45^0, 60^0$ with m=e= $N_t = N_b = 0.1$,Pr=1, $G_t = 1, G_c = 0.1$.

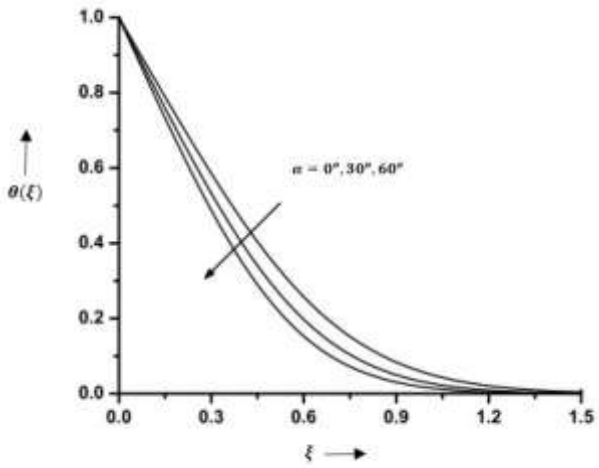

Variation of t(ξ)) vs ξ on different values of $\alpha = 30^0, 45^0, 60^0$ with m=e= $N_t = N_b = 0.1$,Pr=1, $G_t = 1, G_c = 0.1$.

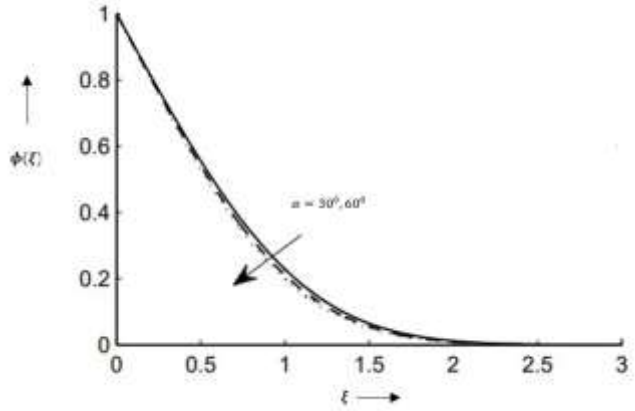

Variation of $\varphi(\xi)$ vs ξ on different values of $\alpha = 30^0, 45^0, 60^0$ with m=e= $N_t = N_b = 0.1$,Pr=1, $G_t = 1, G_c = 0.1$.

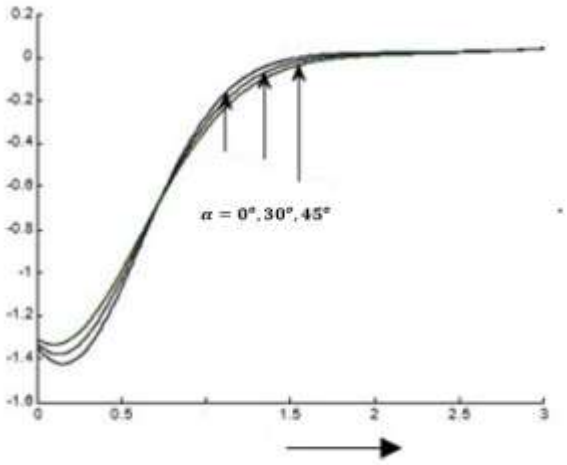

Variation of $-t'(\xi)$ vs ξ on different values of $\alpha = 30^0, 45^0, 60^0$ with m=e= $N_t = N_b = 0.1$, Pr=1, $G_t = 1, G_c = 0.1$

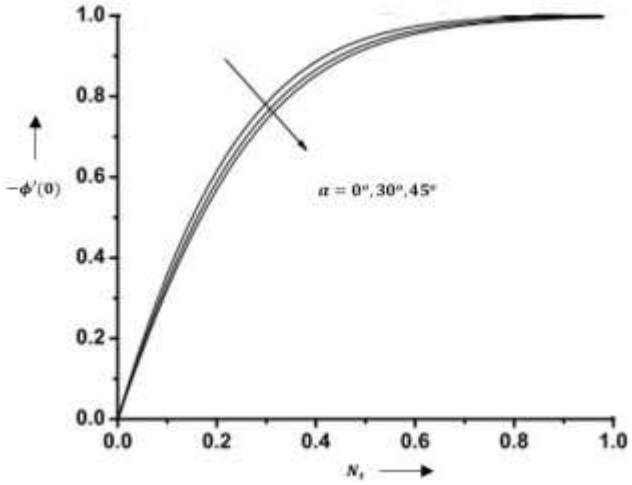

Variation of $-\varphi'(0)$ vs ξ on different values of $\alpha = 30^0, 45^0, 60^0$ with m=e= $N_t = N_b = 0.1$,Pr=1, $G_t = 1, G_c = 0.1$.

Figures 5-10 shows that the effect of the inclined angle α on the velocity, skin friction, temperature, concentration profile, Nusselt number and Sherwood number. Skin friction, temperature profile,

concentration profile and Sherwood number decreasing with increasing the value of α while velocity profile and Nusselt number decreasing. This behavior can be explained by the changes in heat transfer mechanisms associated with the inclined surface. A higher angle of inclination can result in less effective convective heat transfer as the flow becomes less aligned with the temperature gradient. The reduced interaction between the fluid and the heated surface results in lower thermal energy retention within the boundary layer, leading to a diminished temperature profile.

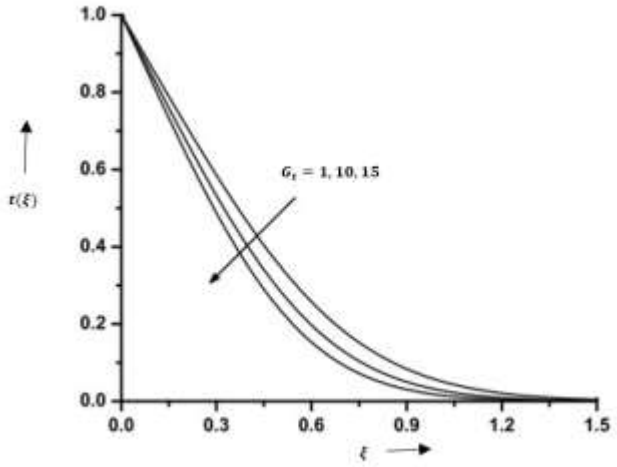

Variation of $t(\xi)$ vs ξ on different values of G_t with m=e= $N_t = N_b = 0.1$,Pr=1, $G_c = 0.1$.

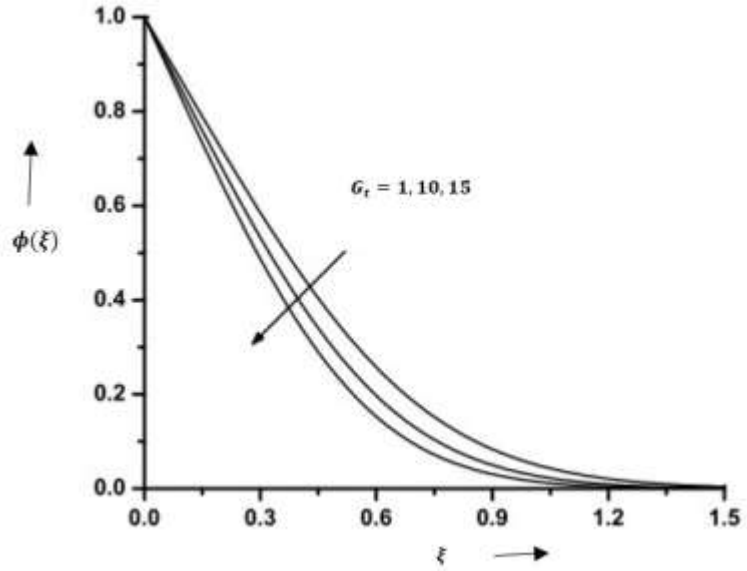

Variation of $\varphi(\xi)$ vs ξ on different values of G_t with m=e = $N_t = N_b = 0.1$,Pr=1, $G_c = 0.1$.
Figures 11-12 showing the effect of G_t. Figures 11 and 12 demonstrate that as the thermal Grashof number G_t increases, the temperature profile rises due to enhanced buoyancy effects and improved convective heat transfer, while the concentration profile decreases due to intensified mixing and disruption of concentration gradients. These findings highlight the critical interplay between thermal and mass transfer processes within the fluid system and underscore the importance of buoyancy-driven flows in influencing temperature and concentration distributions in various engineering applications.

CONCLUSION:

In the context of a numerical study examining mixed convection over a stretching sheet in the presence of a free stream and a magnetic field, it has been observed that the governing equations of the flow exhibit dual solutions. This duality in solutions highlights the complexity of the flow behavior under the influence of multiple physical forces, such as buoyancy and magnetic effects. The first solution, which aligns with physical observations, reflects realistic fluid behavior and demonstrates stable flow characteristics. This solution is characterized by moderate fluid velocities and follows the expected patterns of heat and mass transfer in mixed convection scenarios. The presence of the stretching sheet and the external magnetic field contributes to the dynamics of the flow, facilitating the development of a thermal boundary layer and influencing the overall convective heat transfer.

In contrast, the second solution diverges significantly from physical reality. This solution is characterized by excessively high fluid velocities that are not feasible within the context of the system being studied. Such unrealistic velocities suggest that the second solution may stem from mathematical anomalies or instability in the governing equations rather than representing a viable physical state. This discrepancy highlights the importance of critically evaluating solutions derived from mathematical models, particularly when dual solutions arise.

REFERENCES:

1. Ahmed, N.& Khan, N. (2000): Boundary layer flow past a stretching plate with suction and heat transfer with variable conductivity. IJEMS, Vol.7(1), pp.51-53.
2. Aman S., Mdallal Q, Khan I., (2020): Heat transfer and 2nd order slip effect on MHD flow of fractional Maxwell fluid in a porous medium. Int. Journal of King Saud University Science, 32(1), pp.450–458.
3. Bhargava R, Sharma S, et al. (2007): Numerical Solutions for Micropolar Transport Phenomena Over a Nonlinear Stretching Sheet. Nonlinear Analysis: Modelling and Control, vol.12(1), pp. 45-63.
4. Cao, W., I.L., A., Yook, S., V.A., O., & Ji, X. (2022). Simulation of the dynamics of colloidal mixture of water with various nanoparticles at different levels of partial slip: Ternary-hybrid nanofluid. *International Communications in Heat and Mass Transfer*, *135*, 106069. https://doi.org/10.1016/j.icheatmasstransfer.2022.106069.
5. Choi SUS, Zhang ZG, Yu W, Lockwood FE (2001): Anomalously Thermal Conductivity Enhancement in Nanotube Suspensions. Appl. Phys. Lett. Vol.79, pp. 2252-2254, https://doi.org/10.1063/1.1408272.
6. Cortel, R. (2007): Viscous flow and heat transfer over a nonlinearly stretching sheet. Appl. Math Comput, vol.184(2), pp.864-873, https://doi.org/10.1016/j.amc.2006.06.077.
7. Fang, T. &Yao, S. Zang J.& Aziz A. (2009): Slip MHD viscous flow over a stretching- sheet an exact solution. Commun. Nonlinear Sci. Numer. Simul. Vol.14, pp. 3731-3737, https://doi.org/10.1016/j.cnsns.2009.02.012.
8. Ganesh, N. V., Al-Mdallal, Q. M., & Chamkha, A. J. (2019). A numerical investigation of Newtonian fluid flow with buoyancy, thermal slip of order two and entropy generation. *Case Studies in Thermal Engineering*, *13*, 100376. https://doi.org/10.1016/j.csite.2018.100376.
9. Gangadhar K., Kannan T., Dasaradha R., & Gangadhar K., (2016): Radiation and Viscous Dissipation Effects on Laminar Boundary Layer Flow Nanofluid over a Vertical Plate with a Convective Surface Boundary Condition with Suction. Journal of Applied Fluid Mechanics, vol.9(4), pp. 2097-2103.
10. Gangadhar K., Kannan T., Dasaradha R., & Sakthivel G., (2018): Unsteady free convective boundary layer flow of a nanofluid past a stretching surface using a spectral relaxation method. International Journal of Ambient Energy, vol. 41(6), pp. 609-616. DOI: 10.1080/01430750.2018.1472648.
11. Hamid M, Usman M, Khan Z.H, Ahmad R, Wang W (2019): Dual solutions and stability analysis of flow and heat transfer of Casson fluid over a stretching sheet, Physics Letters A vol. 383 pp.2400–2408. https://doi.org/10.1016/j.physleta.2019.04.050.
12. Hayat T, Khan WA, Abbas SZ, Nadeem.S., (2020): Impact of induced magnetic field on second-grade nanofluid flow past a convectively heated stretching sheet. Applied Nanoscience vol.10, pp.3001–3009.
13. Hayat T., Shafiq A., Alsaedi A., & Shahzad S.A.(2016): Unsteady MHD flow over exponentially stretching sheet with slip conditions. J.Applied Mathematics and Mechanics, volume 37, pp.193–208.
14. Jauhri S, Mishra U, (2022): A Study of MHD Fluid with 2nd order Slip and Thermal Flow Over a Nonlinear Stretching Sheet, International Journal of Applied Mechanics and Engineering, vol. 27(2), pp. 98-114. https://doi.org/10.2478/ijame-2022-0022.
15. Jauhri S, Mishra U, (2023): Numerical investigation of MHD nanofluid considering second-order velocity slip effect over a stretching sheet in porous media, Journal of integrated science & technology, vol.11(2), pp.1-7.

https://pubs.thesciencein.org/journal/index.php/jist/article/download/478/313

16. Jauhri, S., Mishra, U. (2021): Dual solutions of EMHD nanofluid at stretching sheet with mixed convection slip boundary condition. International Journal of Heat and Technology, Vol. 39(6), pp. 1887-1896. https://doi.org/10.18280/ijht.390624.
17. Kalidas Das. (2014): Nanofluid flow over a non-linear permeable stretching sheet with partial slip. Journal of the Egyptian mathematical society. Vol. 23(2), pp. 451-456, https://doi.org/10.1016/j.joems.2014.06.014.
18. Kang, H.U. & Kim S.H. & Oh J.M. (2006): Estimation of thermal conductivity of nanofluid using experimental effective particle volume. Exp. Heat Transfer, vol.19, pp.181–191, https://doi.org/10.1080/08916150600619281.
19. Khan, W.A & Pop I (2010): Boundary-layer flow of a nanofluid past a stretching sheet. Int.J of Heat and Mass Transfer, vol.53, pp.2477-2483. 10.1016/j.ijheatmasstransfer.2010.01.032
20. Li Yi-Xia., Alshbool M., et.al., (2021): Heat and mass transfer in MHD Williamson nanofluid flow over an exponentially porous stretching surface. Int. J. Case Studies in Thermal Engineering, Vol. 26, pp. 89-99.
21. Lin Wu (2008): A slip model for rarefied gas flows at arbitrary Knudsen number, Applied Physics Letter vol. 93. http://digitalcommons.unl.edu/mechengfacpub/127.
22. Norfifah B et.al (2016): Stability of Dual Solutions in Boundary Layer Flow and Heat Transfer on a Moving Plate in a Copper-Water Nanofluid with Slip Effect, WSEAS Transaction on Fluid Mechanics, Vol. 11, pp.151-158. 10.17485/ijst/2016/v9i48/97740.
23. Rafique K, Alotaibi H., et al.(2020): Numerical Solutions of Micropolar Nanofluid over an Inclined Surface Using Keller Box Analysis. Int. Journal of mathematics, vol(2020),pp. 975-985.
24. Sakthivel G., (2018): Boundary layer flow of nanofluids to analyse the heat absorption/generation over a stretching sheet with variable suction/injection in the presence of viscous dissipation. International Journal of Ambient Energy, vol 41(9), pp. 969-980. DOI: 10.1080/01430750.2018.1501738.
25. Sharma, Rohit, Raju, Chakravarthula S., Animasaun, Isaac L., Santhosh, Halavudara B. and Mishra, Manoj K., (2021): Insight into the significance of Joule dissipation, thermal jump and partial slip: Dynamics of unsteady ethelene glycol conveying graphene nanoparticles through porous medium" *Nonlinear Engineering*, vol. 10(1), pp. 16-27. https://doi.org/10.1515/nleng-2021-0002
26. Song, Y., Obideyi, B., Shah, N. A., Animasaun, I., Mahrous, Y., & Chung, J. D. (2021). Significance of haphazard motion and thermal migration of alumina and copper nanoparticles across the dynamics of water and ethylene glycol on a convectively heated surface. *Case Studies in Thermal Engineering*, *26*, 101050. https://doi.org/10.1016/j.csite.2021.101050.
27. Wang, F., Ahmad, S., Al Mdallal, Q. *et al.* Natural bio-convective flow of Maxwell nanofluid over an exponentially stretching surface with slip effect and convective boundary condition. *Sci Rep* **12**, 2220 (2022). https://doi.org/10.1038/s41598-022-04948-y.
28. Wenhao Cao, Animasaun I.L., Se-Jin Yook, Oladipupo V.A., Xianjun Ji., (2022): Simulation of the dynamics of colloidal mixture of water with various nanoparticles at different levels of partial slip: Ternary-hybrid nanofluid, International Communications in Heat and Mass Transfer, Vol. 135,https://doi.org/10.1016/j.icheatmasstransfer.2022.106069.
29. Zeng Z, Grigg R (2006): A Criterion for Non-Darcy Flow in Porous Media. Transport in Porous Media, vol. (53), pp. 57-69. DOI 10.100